STRUCTURAL BEHAVIOR OF COMPOSITE GIRDERS CONSISTING OF HYBRID FRP I-BEAMS AND PRECAST ULTRA-HIGH-STRENGTH FIBER REINFORCED CONCRETE SLABS

S.V.T. Janaka PERERA[1], Hiroshi MUTSUYOSHI[2] and N. Duc HAI[3]

[1]Member of JSCE, Postdoctoral Research Fellow, Dept. of Civil and Env. Eng., Saitama University
(255 Shimo Okubo, Sakura-ku, Saitama 338-8570, Japan)
E-mail:janaka@mail.saitama-u.ac.jp
[2]Member of JSCE, Professor, Dept. of Civil Env. Eng., Saitama University
(255 Shimo Okubo, Sakura-ku, Saitama 338-8570, Japan)
E-mail:mutuyosi@mail.saitama-u.ac.jp
[3]Postdoctoral Research Fellow, Dept. of Civil Eng., Marshall University
(Marshall University, Huntington, West Virginia, U.S.A.)
E-mail:nguyenhai@marshall.edu

Fiber reinforced polymer (FRP) has recently been utilized in the construction of many pedestrian and road bridges due to its light weight, high specific strength, and corrosion resistance. This beam optimizes the combined use of carbon-fiber reinforced polymer (CFRP) and glass-fiber reinforced polymer (GFRP) in a single wide-flange beam section. While CFRP has high tensile strength and stiffness, it is relatively expensive whereas GFRP is comparatively less expensive, but its mechanical properties are lower than those of CFRP. Hybrid Fiber Reinforced Polymer (HFRP) has several advantages such as a light weight, high specific strength, and corrosion resistance. This material is expected to find its application in severe corrosive environments or where light-weight rapid construction is required. This paper presents the development of composite girders using HFRP I-beams and precast Ultra-High Strength Fiber Reinforced Concrete (UHSFRC) slabs. UHSFRC has high strength and high ductility allowing for a reduction in the cross-sectional area and self weight of the girder. A number of full-scale flexural beam tests were conducted using different slab dimensions and with/without epoxy bonding between the slab and HFRP I-beam. The test results suggested that the flexural stiffness of composite girders with the combined use of bolts and epoxy bonding as shear connectors is higher than those with only bolt-connectors. Delamination failure was not observed in the compressive flange of the HFRP I-beam and the high tensile strength of CFRP in the bottom flange was effectively utilized with the addition of the UHSFRC slab on the top flange.

Key Words : *composite girder; hybrid fiber reinforced polymer; ultra-high performance fiber-reinforced concrete; flexural stiffness*

1. INTRODUCTION

Fiber reinforced polymer (FRP) has recently been adopted in many pedestrian and road bridges due to its light weight, high specific strength, and corrosion resistance. Presently, a hybrid FRP (HFRP) beam for bridge girder applications is being developed. This beam optimizes the combined use of carbon fiber reinforced polymer (CFRP) and glass fiber reinforced polymer (GFRP) in a single wide-flange beam section[1)].

While CFRP has high tensile strength and stiffness, it is relatively expensive, whereas GFRP is comparatively less expensive but its mechanical properties are lower than those of CFRP. In a beam subjected to bending moment about the strong axis, the top and bottom flanges are subjected to high axial stress while the web is subjected to shear stress. In the HFRP beam, the flanges are fabricated using a combination of CFRP and GFRP layers. On the other hand, the web is composed entirely of GFRP because it is not subjected to the same high stresses. The HFRP beam therefore utilizes the advantages of both CFRP and GFRP for strength, stiffness and economy.

The HFRP beam is expected to find its application in severe corrosive environments or where lightweight rapid construction is required.The application of HFRP composites could also contribute to a reduction of life cycle costs (LCC) of the structure and environmental load due to its low carbon dioxide emission[2, 3].

According to past studies, GFRP beams fail due to delamination of the top flanges[1, 4]. However, a past study has shown that a topping slab prevents the top flange delamination of GFRP beams due to compressive stress[4]. Ultra-high strength fiber reinforced concrete (UHSFRC) is being used in topping slabs because it enables the use of smaller cross-section and durability.

Therefore, the purpose of this paper is to present the flexural behavior of pultruded HFRP beams with a topping slab. Precast UHSFRC was used for the topping slab.

2. EXPERIMENTAL PROGRAM

(1) Materials

The HFRP I-beams were manufactured using the pultrusion process using the FRP layer composition shown in Table 1. The top and bottom flanges of the I-beam were composed of CFRP and GFRP in order to increase flexural strength and beam stiffness. All CFRP fibers in the flanges were aligned longitudinally (oriented at 0 degrees) while the GFRP was oriented at 0, 90 and ±45 degrees to provide integrity across the flange width and to avoid strong anisotropic behavior. The web was composed entirely of GFRP because of the lower stresses and to reduce cost. The overall height of the HFRP beam was 250 mm and the flange width was 95 mm. The flange thickness was 14 mm and the web thickness was 9 mm as shown in Fig. 1. The mechanical properties of CFRP and GFRP are listed in Table 1. The effective mechanical properties of the HFRP laminates obtained from the material tests are listed in Table 2.

Mixture proportions of the UHSFRC are listed in Table 3. The UHSFRC is composed of water, premixed cementitious powder, sand, water reducing agent and steel fibers. The premixed cementitious powder includes ordinary Portland cement, pozzolanic materials (usually silica fume) and ettringite according to Japanese standards for blended cement. The steel fibers have a tensile strength of 2,000 N/mm^2 and lengths of 22 mm and 15 mm. The fibers were added at approximately 1.75% volume ratio. The UHSFRC slabs were precast and cured at 85 °C for 24 hours.

Table 1 Mechanical properties of materials

Parameters		CFRP 0°	GFRP 0/90°	GFRP ±45°	GFRP CSM[a]
Volume Fraction (%)		55	53	53	25
Volume Content (%)	Flange	33	17	41	9
	Web	0	43	43	14
Young's Modulus (kN/mm^2)	E_{11}	128.1	25.9	11.1	11.1
	E_{22}	14.9	25.9	11.1	11.1
Shear Modulus (kN/mm^2)	G_{12}	5.5	4.4	10.9	4.2
Poisson's Ratio (mm/mm)	ν_{12}	0.32	0.12	0.58	0.31

[a] CSM = Continuous Strand Mat

Compression tests were performed on 100×200 mm cylinders of the UHSFRC to determine compressive strength and modulus of elasticity. Moduli of rupture tests were performed on 100×100×400 mm specimens to determine the tensile strength of the UHSFRC. Three specimens were tested for each material property and the average values are listed in Table 4.

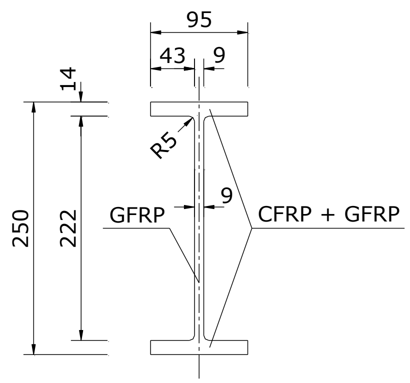

Fig. 1 Dimensions of HFRP I-beams (unit: mm)

Table 2 Effective Mechanical Properties of HFRP Laminates

Property	Flange	Web
Compressive strength (N/mm^2)	394	299
Tensile strength (N/mm^2)	884	185
Young's modulus (kN/mm^2)	49.6	17.8

Table 3 Mix Proportions of UHSFRC

Air content (%)	Unit quantity (kg/m^3)				Steel fiber (kg/m^3)
	Water	Premix cement	Sand	W.R.A[a]	
2.0	205	1,287	898	32.2	137.4

[a] W.R.A = Water Ratio Admixture

Table 4 Test Results of UHSFRC Material

Compressive strength (N/mm^2)	Tensile strength (N/mm^2)	Young's modulus (kN/mm^2)
173	14.3	48.6

(2) Test variables

The test variables for the full-scale beam flexural tests are listed in Table 5. Five specimens with different dimensions for the UHSFRC slab were tested. The geometry of the test specimens and the dimensions of the beam cross-sections are shown in Figs. 2 and 3. The total length of each specimen was 3,500 mm with the flexural and shear spans at 1,000 mm as shown in Fig. 2. Timber stiffeners were installed at a spacing of 500 mm on both sides of the web to prevent web buckling. The stiffeners were bonded to the HFRP specimens using epoxy bonding. Different types of shear connectors including headed bolts with/without epoxy bonding and slab anchors were tested to investigate the composite/non-composite actions between the HFRP beam and the UHSFRC slab (Fig. 3). The spacing of headed bolts and slab anchors was determined from the shear connection tests to prevent premature bolt shear failure as shown in Fig. 4. A torque wrench was used to apply 20 Nm torque to the bolts in all specimens.

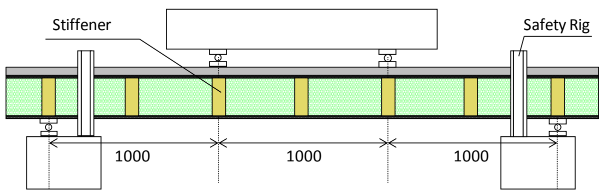

Fig. 2 Geometry of specimen for flexural test (unit: mm)

(3) Experimental setup and procedure

A four-point bending test was conducted on all specimens. The experimental setup is shown in Fig. 2. The load was applied by a manually-operated hydraulic jack until beam failure. The applied load, deflection at mid-span, and strains in the HFRP beam section were measured throughout the test.

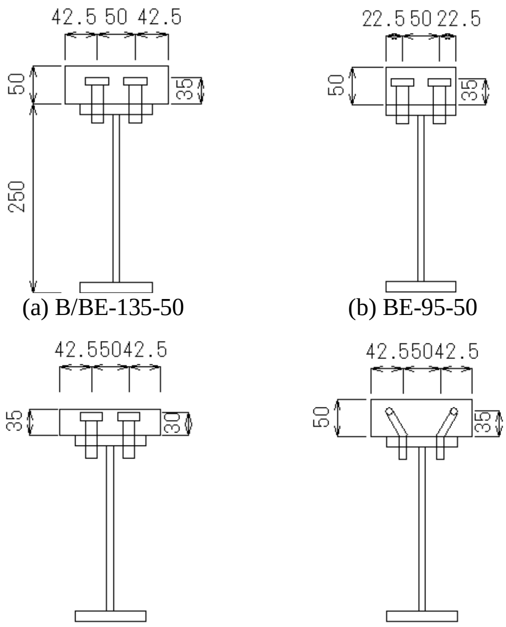

(a) B/BE-135-50 (b) BE-95-50 (c) BE-135-35 (d) SA-135-50

Fig. 3 Dimensions of the beam cross-sections (unit: mm)

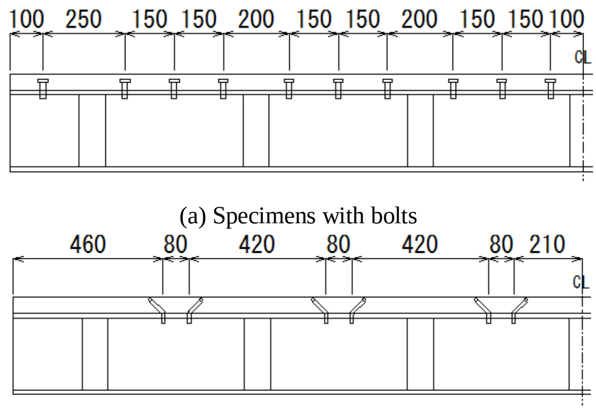

(a) Specimens with bolts

(b) Specimen with slab anchors

Fig. 4 Locations of shear connectors (unit: mm)

Table 5 Flexural Beam Test Variables

Specimen name	Shear Connector	EB[a]	W[b] (mm)	T[c] (mm)	EL[d] (mm)
B-135-50	M16 bolt	No	135	50	35
SA-135-50	Slab anchor M10	No	135	50	35
BE-95-50	M16 bolt	Yes	95	50	35
BE-135-35	M16 bolt	Yes	135	35	30
BE-135-50	M16 bolt	Yes	135	50	35

[a] EB = Epoxy bonding; [b] W = Width of UHSFRC slab; [c] T = Thickness of UHSFRC slab; [d] EL = Embedded length of bolt

3. TEST RESULTS AND DISCUSSION

Figure 5 shows the relationship between the load and mid-span deflection of the pultruded I-beam. It can be seen that the behavior of the beam is almost linear up to the failure. The typical failure mode of pultruded beams is shown in Figs. 6 and 7. There was crushing of fibers near the loading point due to load concentration followed by delamination of the compressive flange between the upper and lower part of the top flange. It seems that the load carrying capacity of the pultruded I-beam is not governed by the compressive or tensile strength of the FRP material, but related to the bonding strength at the interface between fiber layers.

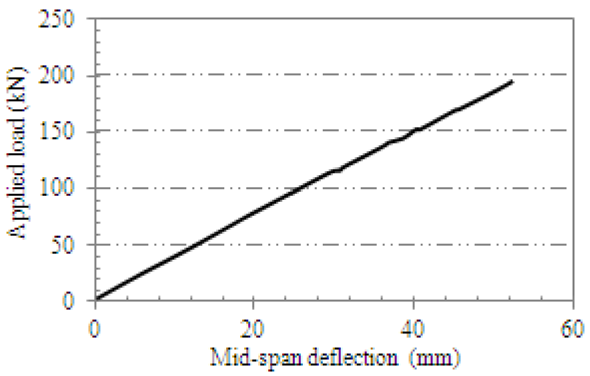

Fig. 5 Load-deflection curve at mid-span section

Figure 8 shows the relationship between load and longitudinal strain at the top and bottom flange at the mid-span section. The results indicate that both compressive and tensile strain behave linearly until failure. Both maximum compressive and tensile strains reach a value of approximately 6,100 x 10^{-6} mm/mm which is only 44% of the ultimate tensile strain of CFRP.

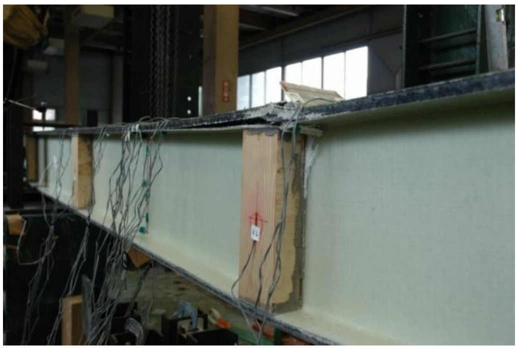

Fig. 6 Crushing of fibers and delamination

Fig. 7 Closer view of delamination

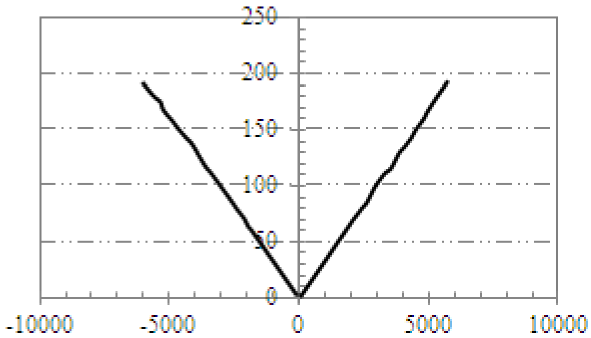

Fig. 8 Load-longitudinal strain curve

Figure 9 shows the load and mid-span deflection relationship of each specimen. For comparison, the load-deflection relation curve for a HFRP beam without UHSFRC slab (control specimen) is also included in Fig. 9. All specimens with bolt shear connectors show higher stiffness and loading carrying capacity than the control specimen. In particular, the stiffness of specimen BE-135-50 is approximately 15% higher compared with that of specimen B-135-50. On the other hand, specimen SA-135-50 did not perform well compared to the specimens using headed bolts.

Figure 10 shows the position of the strain gauges through the depth of the composite girder mid-sapn section. Figure 11 shows the relationship between the load and longitudinal strain through the depth of the composite girder at mid-span section for various load levels, including failure load. The specimen with epoxy bonding (Fig. 11a) shows a linear strain distribution through the cross-section. On the other hand, Figs. 11b and 11c show slipping at the interface between the UHSFRC slab and the HFRP beam for the specimen without epoxy bonding. This result indicates that specimens with bolted and bonded connections show full composite action until the final failure. The specimen with shear anchors showed even larger slip than the specimens with bolts. The results also show that at failure, the maximum tensile strain recorded at the tensile flange of the HFRP was approximately 10,000 μ. This level of strain is significantly higher than the 6,000 μ recorded at failure in the tensile flange of the HFRP beam tested without a slab. This shows that the addition of an UHSFRC slab on the HFRP beam resulted in the effective utilization of the high tensile strength of the CFRP.

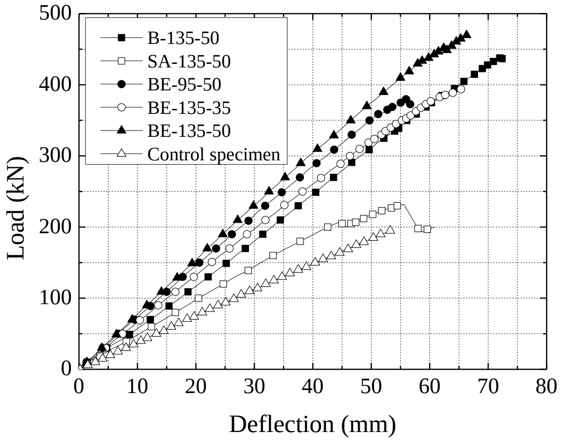

Fig. 9 Load-deflection relationships

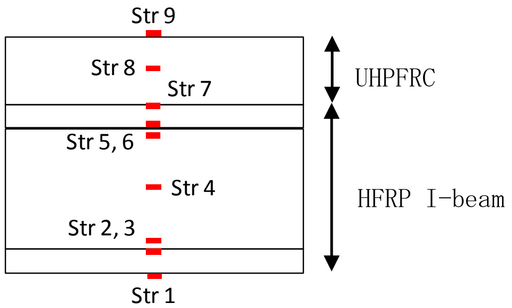

Fig. 10 Positions of strain gages through the depth of the composite girder at mid-span section

Figure 12a shows the position of strain gauges in HFRP top flange near a bolt. The strain distributions along the top flange of the HFRP beam near a bolt hole in the left shear span are shown in Fig. 12. As shown in Fig. 12a, for a specimen without epoxy, the strain to the right of the bolt is small while strain to the left of the bolt shows high compression in the HFRP beam flange. This strain distribution indicates that slipping occurred at the interface between the UHSFRC slab and the HFRP beam allowing the bolts to bear against the edge of the hole to resist the horizontal shear flow. On the other hand, this behavior was not observed in specimens with epoxy bonding. Figure 12b shows that the strains in the HFRP beam flange are uniformly distributed regardless of the bolt types and bolt hole location. These results confirm that the slipping between the UHSFRC slab and the HFRP beam was resisted by the epoxy bonding especially in the shear span where horizontal shear stress is significant. The bolts also serve to prevent peeling at the UHSFRC slab to HFRP beam interface, and to provide reserve strength if debonding occurs.

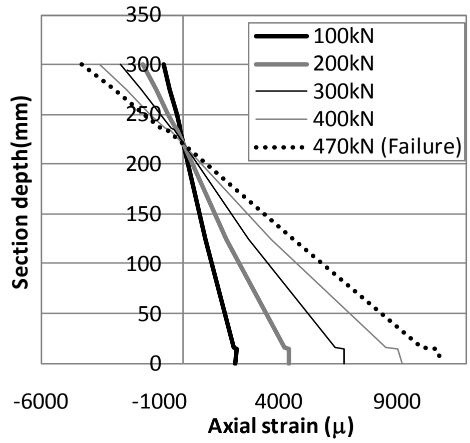

(a) BE-135-50

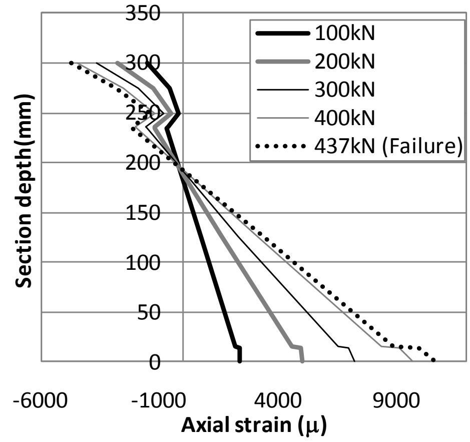

(b) B-135-50

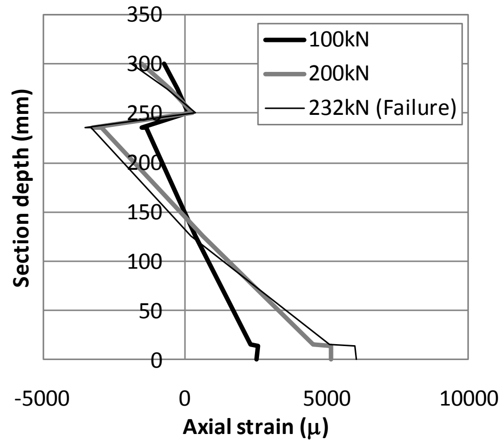

(c) SA-135-50

Fig. 11 Longitudinal strain distribution along the depth of the composite girder

All specimens with headed bolts failed due to crushing of the UHSFRC slab at the loading point followed by crushing of the HFRP beam flange as shown in Fig. 13a. Delamination of the top flange of the HFRP beam was observed in specimen SA-135-50 with shear anchors (Fig. 13b). This failure mode is similar to that of HFRP beams without a slab; however, the failure was not brittle as the UHSFRC slab carried compressive force even after delamination failure occurred. In addition, a few of the slab anchors failed in shear, while the others caused bearing failure in the HFRP beam flange.

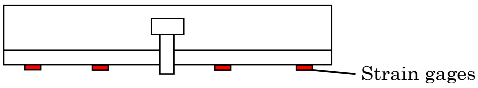

(a) Position of strain gauges

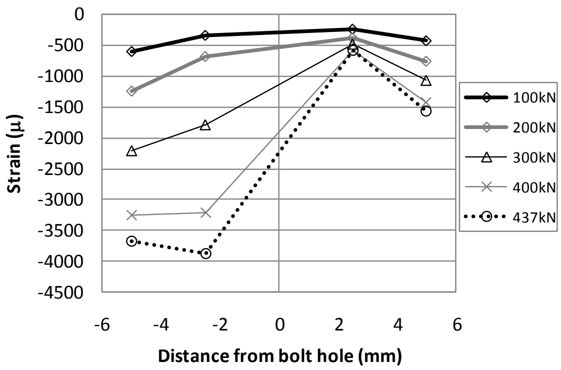

(b) Specimen without epoxy

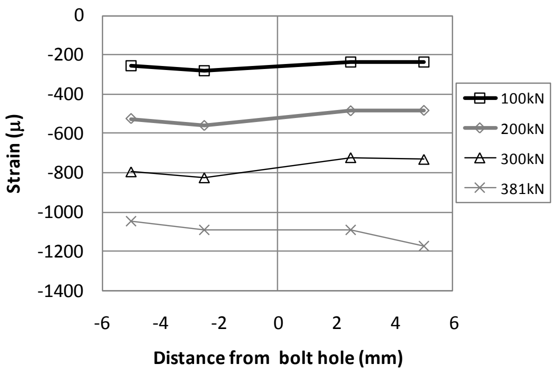

(c) Specimen with epoxy

Fig. 12 Strain distribution in HFRP top flange near bolt hole

Fiber model analysis of the HFRP-UHSFRC composite girders was conducted and the results were compared with the experimental results. Bernoulli-Euler theory was assumed in this analysis. A bi-linear stress-strain relationship from the design code for ultra-high-strength fiber reinforced concrete structures (Fig. 14) was used to model UHSFRC[5].

Table 6 shows comparisons between analytical and experimental results for the HFRP-UHSFRC composite girders that used headed bolt and epoxy bonding as shear connectors. The results indicated that the analytical model could well predict the failure load and failure mode of beams. The differences in failure load between the analysis and experiment are less than 5%. However, the analytical model over-estimates the stiffness of the composite girder as shown in Fig. 15. According to the analytical model, compression failure of the UHSFRC slab should occur at mid-span. However, failure occurred at the loading point in the experiment and higher strains were recorded at the loading point due to stress concentration. The disagreement in stiffness between the analytical and experimental results is attributed in part to early plastic behavior at the loading point caused by this stress concentration. The analytical model assumes perfect bond between the UHSFRC and HFRP, whereas the test specimens may experience some deformation at the bond interface.

(a) Crushing of UHSFRC slab

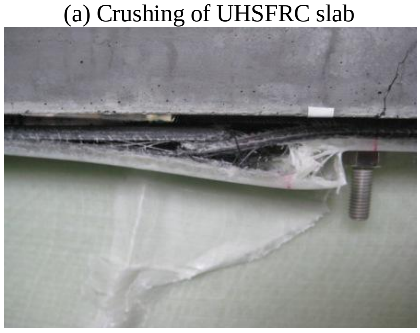

(b) HFRP flange delamination failure

Fig. 13 Failure modes of composite girders in flexure

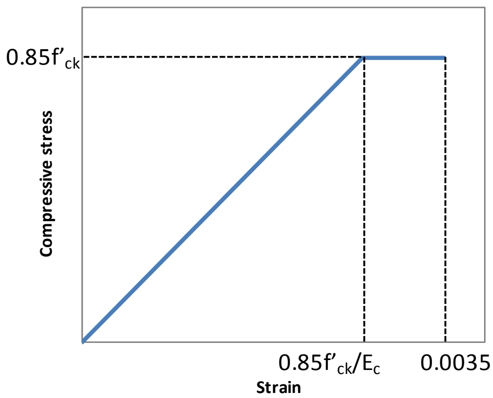

Fig. 14 Bi-linear stress-strain relationship of UHSFRC

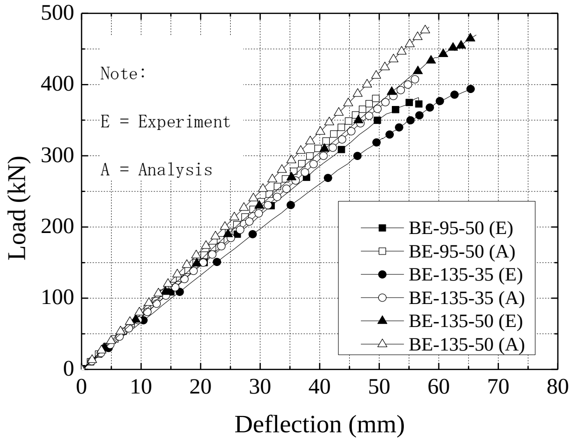

Fig. 15 Comparisons of load-defection curves between experiments and analysis

Table 6 Flexural Beam Test Results at Failure

Beam	Predicted failure load (kN)	Actual failure load (kN)	Predicted/actual failure mode
B-135-50	—	438	Compression (UHSFRC)
SA-135-50	—	232	Delamination (HFRP top flange)
BE-95-50	384	382	Compression (UHSFRC)
BE-135-35	411	394	Compression (UHSFRC)
BE-135-50	481	470	Compression (UHSFRC)

4. CONCLUSIONS

This paper presents an experimental study of HFRP beams and composite girders consisting of HFRP beams and concrete topping slabs connected by bolts or slab anchors. The main conclusions from the study are summarized as follows:

1. The investigated HFRP beams behave linearly under flexural load and failed suddenly without forewarning. The failure was the crushing of fibers near the loading point due to load concentration followed by the delamination of the compressive flange between the interface of CFRP and GFRP layers.
2. Composite girders consisting of HFRP beams and concrete topping slabs significantly improve their flexural stiffness and effectively utilize the superior properties of the HFRP materials.
3. HFRP-UHSFRC composite girders with headed bolt shear connectors provide considerable stiffness and increase in strength compared with HFRP beams without concrete topping slab.
4. Composite girders with epoxy bonding between the UHSFRC slab and HFRP beam top flange showed an approximate 15% increase in flexural stiffness than beams connected with bolts only.

ACKNOWLEDGMENT: The authors would like to thank Kajima Corporation for providing Ultra High Performance Fiber Reinforced Concrete "SUQCEM" (Super high-Quality CEmentitious Material).

REFERENCES

1) Hai, N.D., Mutsuyoshi, H., Asamoto, S., and Matsui, T.: Structural Behavior of Hybrid FRP Composite I-Beam, *Journal of Construction and Building Materials*, Vol. 24, pp. 956-969, 2010.
2) Sakai, K.: Environmental Design for Concrete Structures, *Journal of Advanced Concrete Technology*, Vol.3, No.1, pp.17-28, 2005.
3) Tanaka, H., Tazawa, H., Kurita, M., and Shimomura, T.: A Case Study on Life-Cycle Assessment of Environmental Aspect of FRP Structures, *Proceedings of Third International Conference on FRP Composites in Civil Engineering (CICE 2006)*, Florida, USA, pp. 175-178, 2006.
4) Perera, S.V.T.J., Mutsuyoshi, H., and Tomoya, A.: Development of Composite Beams Using Ultra-High Performance Fiber Reinforced Concrete and Fiber Reinforced Polymers, Proc. of JSCE 14th International Summer Symposium, CD-ROM, Nagoya-Japan, 2012.
5) Concrete Committee of Japan Society of Civil Engineers: Recommendations for Design and Construction of Ultra High Strength Fiber Reinforced Concrete Structures, JSCE Guidelines for Concrete No. 9, pp. 1-106, 2004.